



*Earth and Space Science*

Supporting Information for

**The benefits of local regression for quantifying global warming**

David C. Clarke<sup>1</sup>, Mark Richardson<sup>2,3</sup>

<sup>1</sup>Independent Researcher, Montreal, Quebec, Canada

<sup>2</sup>Jet Propulsion Laboratory, California Institute of Technology, USA <sup>3</sup>Joint Institute for Regional Earth Systems Science and Engineering, University of California, Los Angeles, USA

**Contents of this file**

Figures S<sub>4</sub> to S<sub>12</sub>

**Introduction**

- Figures S<sub>4</sub> to S<sub>7</sub> are supplementary to Section 2.2.1 and provide additional information concerning LOESS window size performance.
- Figures S<sub>8</sub> to S<sub>11</sub> are supplementary to Section 2.2.1 and provide additional information concerning the methods used to assess statistical fit uncertainty.

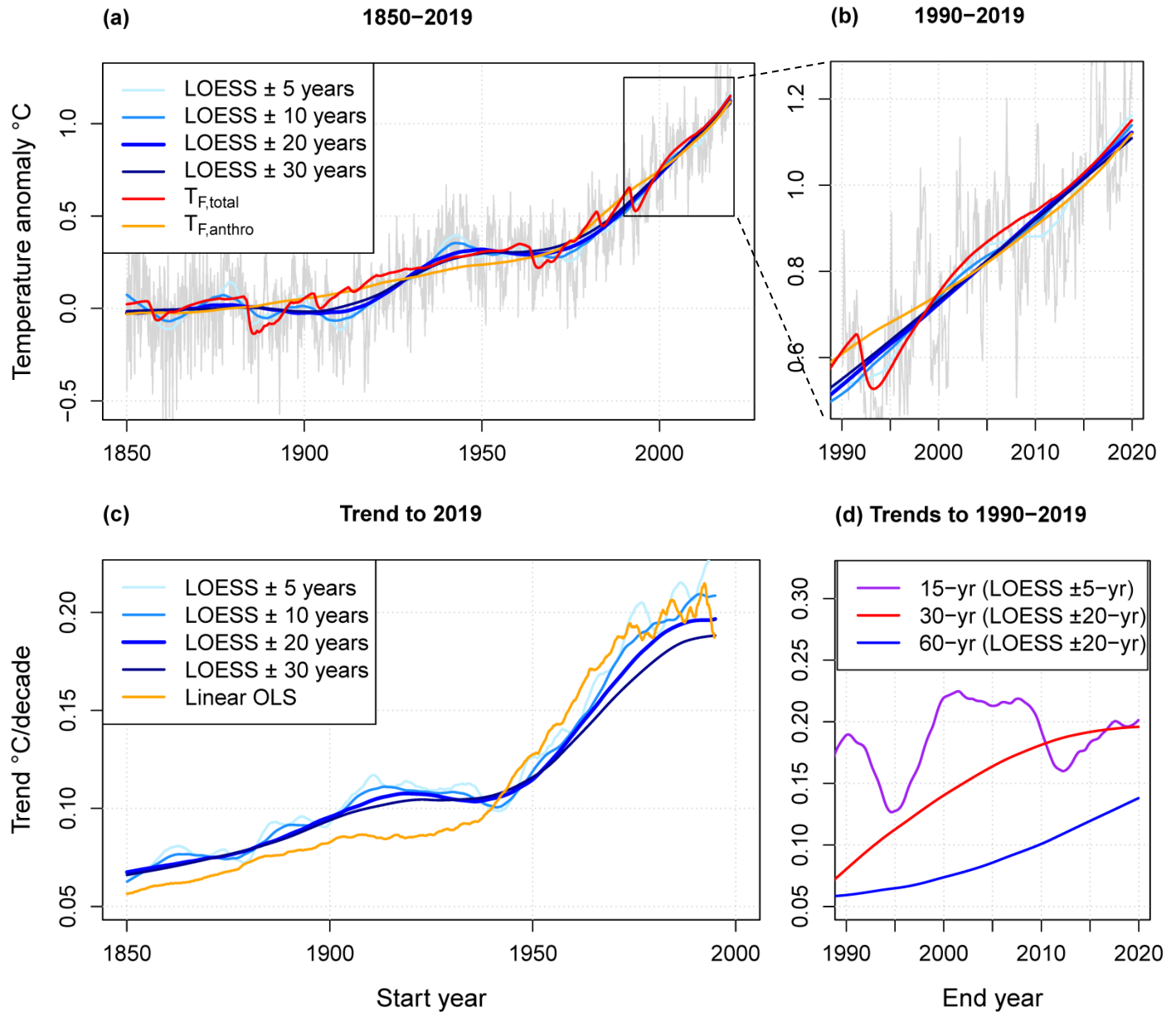


**Figure S4: LOESS window selection and trend methodology.** (a) Cowtan-Way monthly global average temperature series over 1850-2019 (light gray line) is shown with LOESS smooth (blue lines), with windows ranging from  $\pm 30$  years down to  $\pm 5$  years. Also shown are total and anthropogenic forced temperature (red and dark orange lines respectively), estimated from two-box model forced response regressed against Cowtan-Way series following Otto et al. (2015) and Haustein et al. (2017). (b) Same as (a), except over 1990-2019. (c) Overlapping LOESS trends (blue lines) and OLS trends (orange lines) to 2019 are shown, with trend start points of 1850 to 1995. (d) Overlapping fixed length LOESS trends ending in years 1990-2019 are shown.

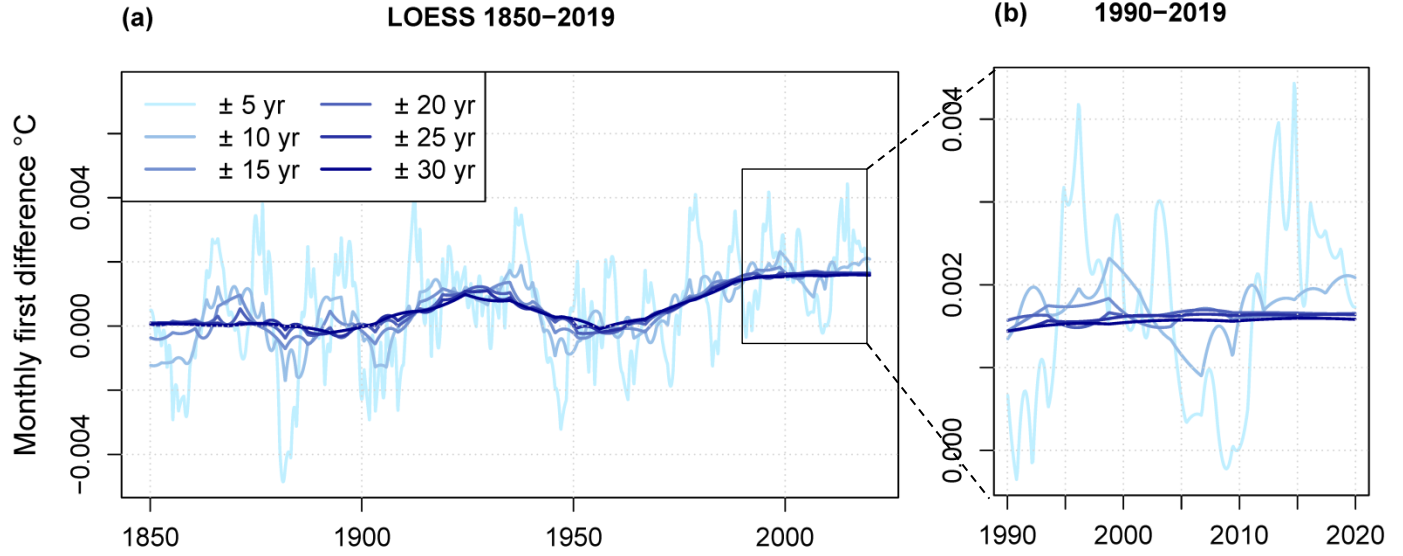


**Figure S5: LOESS window smoothing characteristics.** (a) Monthly first differences over 1850-2019 (light gray line) are shown for LOESS smooths applied to Cowtan-Way temperature series, with windows ranging from  $\pm 5$  years (light blue) to  $\pm 30$  years (dark blue). (b) Same as (a), except over 1990-2019.

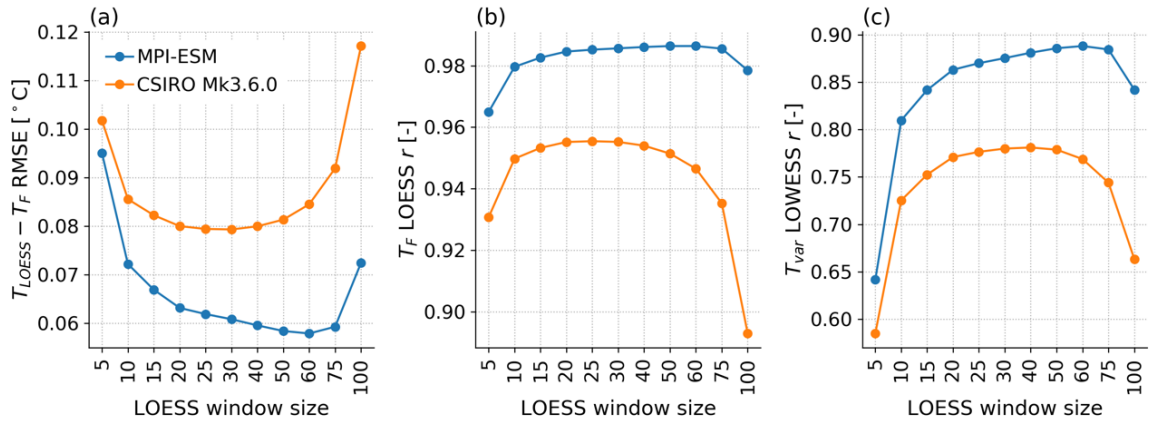


**Figure S6. Large ensemble statistics for non-volcanic year LOESS with different window lengths relative to forced temperature change  $T_F$  (as assessed by ensemble mean at each time step) or their respective residuals (a) RMSE for  $T_F$  versus LOESS, (b) Pearson's  $r$  for LOESS versus  $T_F$ , (c) Pearson's  $r$  for LOESS residuals versus  $T_F$  residuals.**

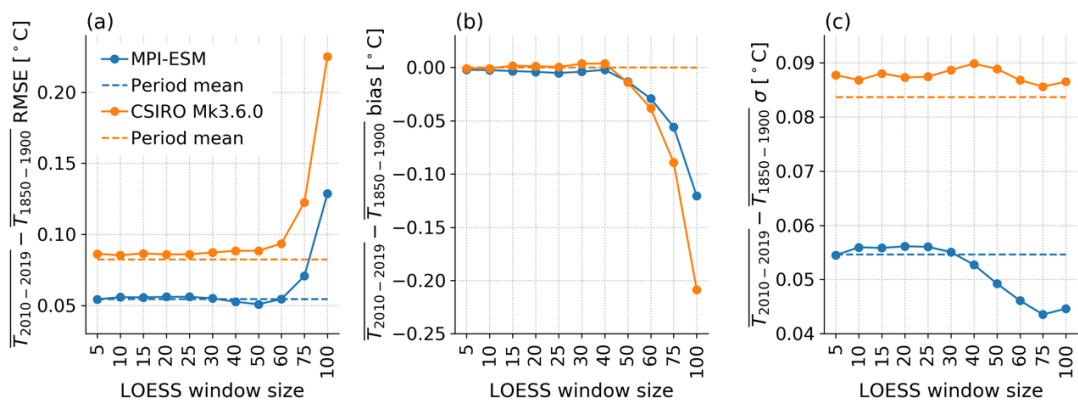


**Figure S7. Ensemble performance statistics for the derived temperature change from 1850—1900 to 2010—2019. The RMSE and bias are calculated relative to the same value calculated from the ensemble mean  $T_F$  estimates. Solid lines with points are from LOESS fits with different window sizes (where a size of 10 is  $\pm 5$  years) and dashed lines are those derived from taking the individual run period mean differences.**

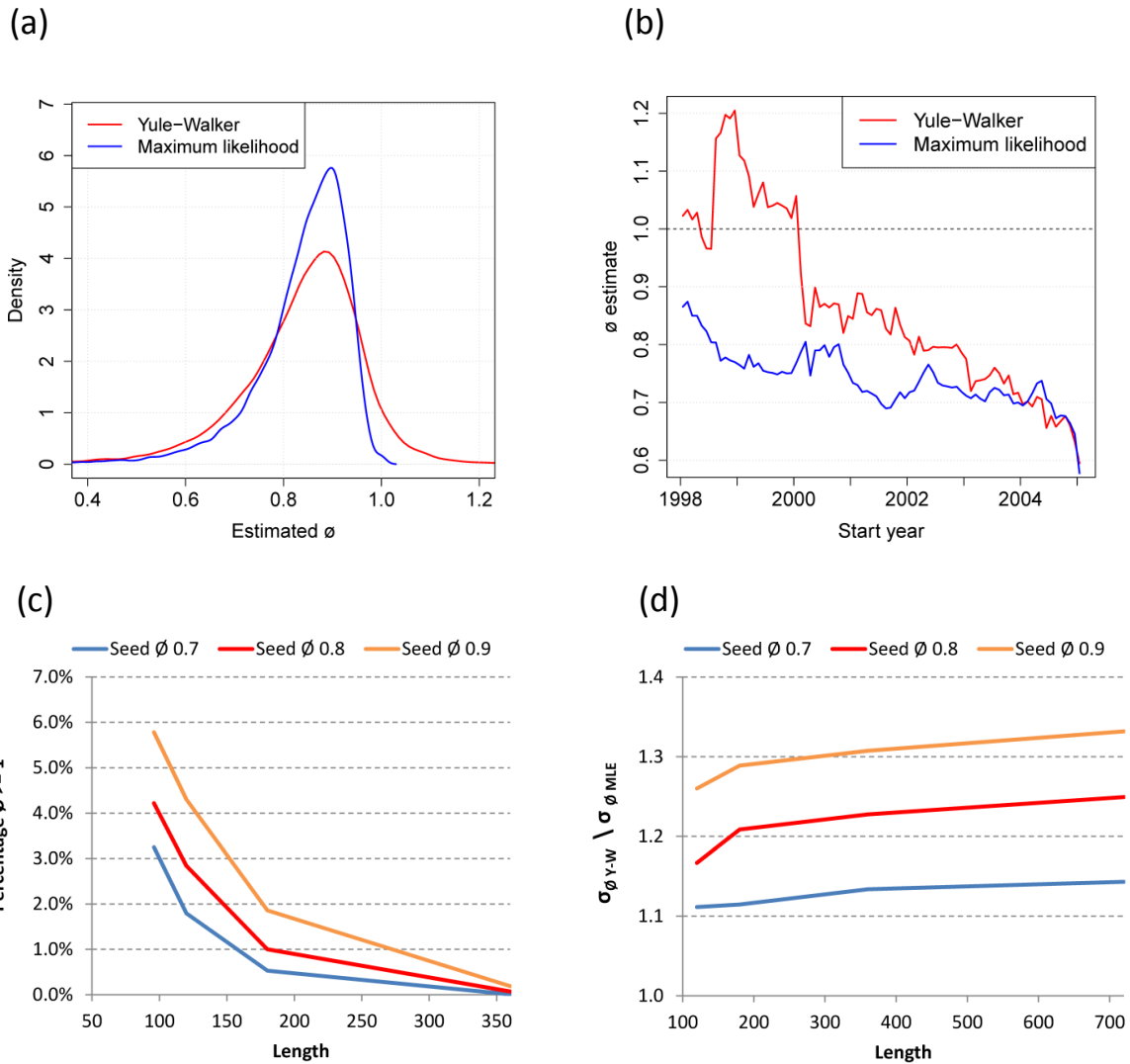


**Figure S8: Yule-Walker (Y-W) vs Maximum Likelihood Estimation (MLE).** (a) PDF of  $\hat{\phi}$  in simulated ARMA(1, 1) 8-year (96-month) series with seed  $\phi = 0.9$ . (b)  $\hat{\phi}$  estimates derived from residuals of 8-year linear trends in Cowtan & Way over 1998-2012. (c) Percentage of simulated series with Y-W  $\hat{\phi} > 1$  by seed and length. (d) Efficiency of MLE relative to Y-W by seed and length .

### ARMA Bias correction and simulated trend coverage

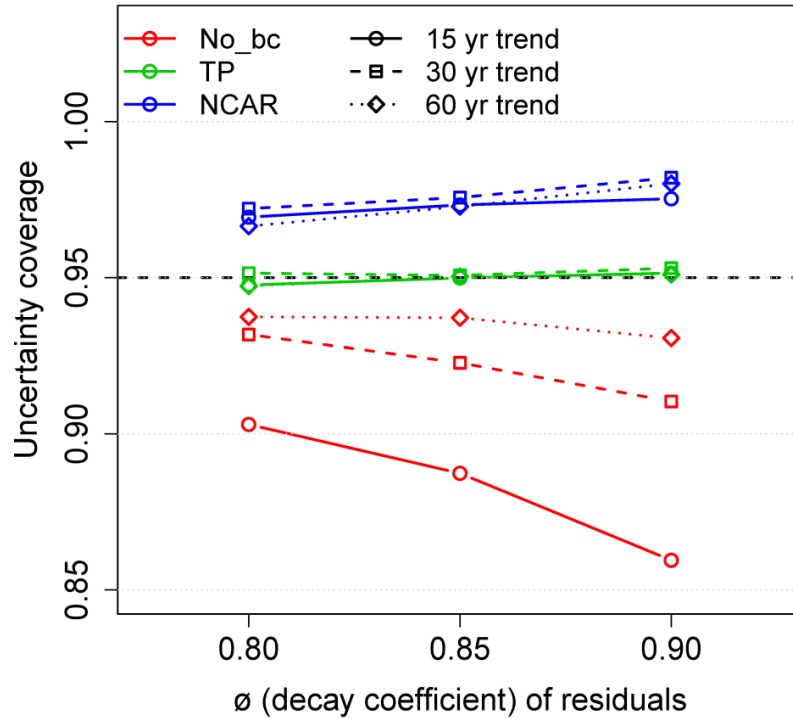


**Figure S9: ARMA (1, 1) bias correction.** Simulated 15-year (solid lines and circles) and 30-year (dashed lines and open circles) trends were generated assuming positively-correlated ARMA(1, 1) noise for three different levels of  $\phi$  (phi) and three different bias correction schemes: No bias correction (red), bias correction derived from Tjøstheim and Paulsen (1996) as used in this study (TP, green), and an alternative bias correction derived from Nychka et al (2001) (NCAR, blue). See section 2.2.2 for details of the bias correction methodology.

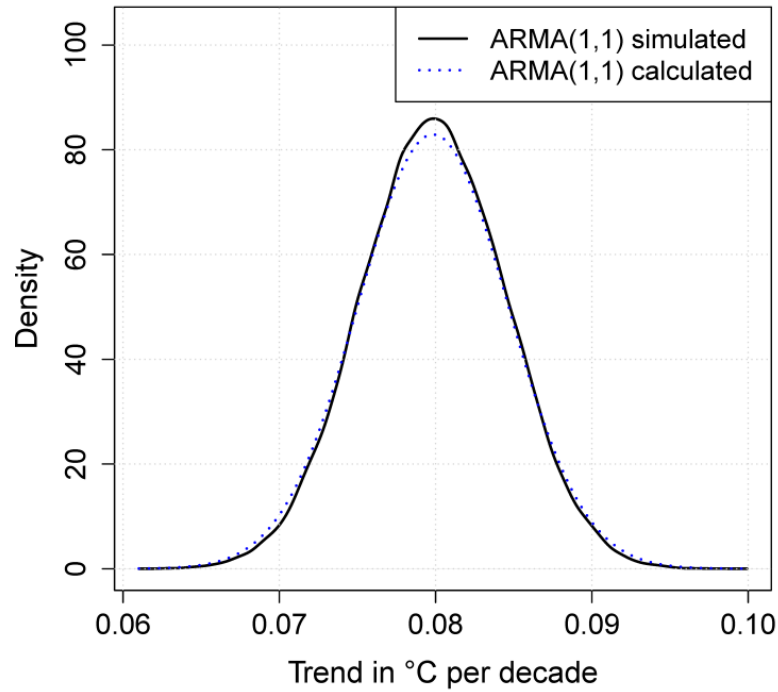


**Figure S10: Uncertainty of LOESS<sub>md</sub> trends.**  $\Delta$ GMST trends over 1880-2019, expressed as change in °C per decade, were simulated by generating a Monte Carlo ensemble of 200K simulations from the Cowtan-Way observational series. Each realization is composed of a central estimate of the trend from Cowtan-Way with added ARMA(1, 1) noise according to the noise model assessed from the fit residuals, as detailed in section 2.2.2. The PDF of the simulated ensemble trend (solid line) is compared to the calculated trend uncertainty (dotted line).

PDF for corrected 2-decade CowtanWay temp rise to 2019

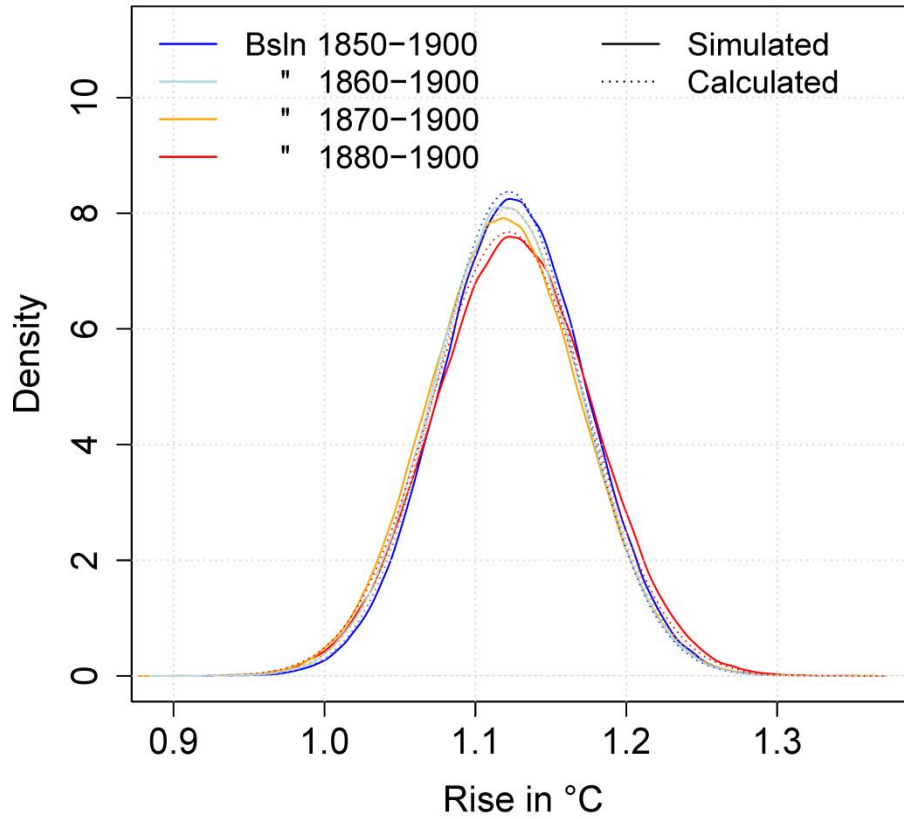


**Figure S11: Uncertainty of  $\text{LOESS}_{\text{bssln}} \Delta\text{GMST}$ .**  $\text{LOESS}_{\text{bssln}} \Delta\text{GMST}$  from various baselines to 2019, expressed as change in  $^{\circ}\text{C}$ , were simulated by generating a Monte Carlo ensemble of 350K simulations from the Cowtan-Way observational series. Each realization is composed of a central estimate of the temperature rise from Cowtan-Way with added  $\text{ARMA}(1, 1)$  noise according to the noise model assessed from the fit residuals, as detailed in section 2.2.2. The PDF of the simulated ensemble trend (solid line) is compared to the calculated uncertainty (dotted line).